Morphology and Mechanical Property of Binary and Ternary Polypropylene Nanocomposites with Nanoclay and $CaCO_3$ Particles

Haibin Chen,[1,2] Mozhen Wang,[1] Yong Lin,[3] Chi-Ming Chan,[3] Jingshen Wu[1,2]

[1]*Department of Mechanical Engineering, The Hong Kong University of Science and Technology, Clear Water Bay, Kowloon, Hong Kong*
[2]*Center for Engineering Materials and Reliability, Fok Ying Tong Graduate School, The Hong Kong University of Science and Technology, Clear Water Bay, Kowloon, Hong Kong*
[3]*Department of Chemcial Engineering, The Hong Kong University of Science and Technology, Clear Water Bay, Kowloon, Hong Kong*

Received 31 May 2007; accepted 5 July 2007
DOI 10.1002/app.27017
Published online 21 August 2007 in Wiley InterScience (www.interscience.wiley.com).

ABSTRACT: Inorganic nanofillers, $CaCO_3$ and nanoclay, are widely applied to improve the mechanical properties of polypropylene (PP). In general, the use of spherical $CaCO_3$ can enhance the impact strength while the use of layered nanoclay can enhance the modulus and yield stress. With the objective to simultaneously improve the stiffness, strength, and impact strength of PP, in this work a ternary nanocomposite, PP/$CaCO_3$/nanoclay (NCPP), was prepared and its morphology, crystallization, and mechanical behaviors were investigated with a comparison to the binary nanocomposites, PP/$CaCO_3$ (CPP) and PP/nanoclay (NPP). The results showed that in NCPP the nanoclay was extremely exfoliated with a much higher degree than that in NPP, which was possibly because the incorporation of $CaCO_3$ nanoparticles adjusted the matrix viscosity and thus provided a balance between shear stress and molecule diffusion. As a result of this highly exfoliated structure, a substantial increase in modulus and yield stress was attained in NCPP. However, its impact strength was less enhanced. The toughening effects of the $CaCO_3$ particles observed in CPP became ineffective. This difference was ascribed to the fact that in NCPP the crystallization behavior was dominated by the nanoclay and the formation of β-phase crystallites induced by the $CaCO_3$ particles was inhibited. J Appl Polym Sci 106: 3409–3416, 2007

Key words: polypropylene; nanocomposites; inorganic fillers; morphology; mechanical properties

INTRODUCTION

Polypropylene (PP), a semicrystalline thermoplastic polymer, has been widely used in different areas such as packaging, textile, household goods, and automobile because of its good processability and attractive cost/performance balance. However, its brittleness, exhibiting at low temperatures or high impact rates as well as its inadequate stiffness, limits its versatile applications. To expand its engineering usage, in the past, extensive efforts have been made to improve its mechanical properties through compounding it with micron- or nanoscaled inorganic particles such as mica, talc, silica, and calcium carbonate.[1–19] Because of the large specific surface area of nanoparticles which leads to strong interfacial interactions with the surrounding polymer matrix, nanoscaled particles are believed to be more effective for the improvement of the mechanical properties of polymers. Among the different nanoparticles, nanoclay is most preferred, since layered silicate sheet in the nanoclay has high aspect ratios ranging from hundreds to thousands. With the use of nanoclay the improvement in mechanical property for a variety of polymers can be achieved at very low filler contents ($\leq$5 wt %), far less than those using traditional micron-scaled fillers (20 $\sim$ 40 wt %).[9–11] The work on PP/nanoclay composites has been extensively reported.[12–16] In general, with the aid of compatibilizer, the PP oligomers modified with either maleic anhydride (MA) or hydroxyl groups (OH), the clay can be well dispersed in the PP matrix in a nanometer scale when using melt-blending techniques. As a result, these PP/clay systems exhibited remarkable enhancements in modulus and tensile strength. However, the impact resistance or fracture toughness was always reportedly decreased or less improved,[14–16] which greatly limits the applications of the PP/clay nanocomposites.

Toughening PP/clay nanocomposites thereby seems to be a challenging subject. Using rubber as toughening modifier for PP is a well-known approach

Correspondence to: J. S. Wu (mejswu@ust.hk).
Contract grant sponsor: Hong Kong Government Research Grant Council; contract grant numbers: HKUST6041/02E, 610960.

Journal of Applied Polymer Science, Vol. 106, 3409–3416 (2007)

where the rubber particles can act as stress concentrators to initiate and terminate crazes and undergo internal cavitation to relieve the triaxial stress state in front of the crack tip, which facilitates shear yielding of the PP matrix.[17] The occurrence of these toughening mechanisms can enhance the fracture toughness substantially. Works with the use of rubber as toughening modifier for PP/clay systems have already been carried out.[18,19] However, the results showed that the improvement in toughness was always accompanied with a loss of modulus and tensile strength. Using rigid particles with low aspect ratios, such as spherical $CaCO_3$ and SiO_2 particles, have been demonstrated to be an alternative way for toughening PP.[3–7] For instance, in the work done by Chan et al.,[5] where nanosized $CaCO_3$ particles were used, a threefold increase in impact strength and a fivefold increase in fracture toughness in terms of J_{IC} were found. The authors proposed that the $CaCO_3$ nanoparticles acted as stress concentrators to promote toughening mechanisms including cavitation and massive plastic deformation of the matrix. Despite the remarkable toughening effect, the spherical particles exhibited a less significant reinforcing role compared to nanoclay, which was ascribed to their different aspect ratios. To simultaneously improve the modulus, yield stress, as well as impact resistance, compounding the PP with rigid particles with different aspect ratios seems to be a possible way. In this work, a ternary PP-based nanocomposite with nanoclay and nanosized $CaCO_3$ particles was prepared. For comparisons, binary nanocomposites, namely PP/$CaCO_3$ and PP/nanoclay, were also prepared and investigated.

EXPERIMENTAL

Materials and nanocomposite preparation

PP homopolymer (cosmoplene Y101) with a melt flow index of 14.5 g/10 min was supplied by the Polyolefin Company PTE (Singapore). Maleic anhydride-modified PP (MA-PP) (Eastman Epolene G-3003) with a molecular weight of 52 kg/mol and a MA content of 0.8 wt % was used as compatibilizer. Montmorillonite clay modified with a quaternary ammonium salt (Cloisite 20A) was received from Southern Clay Products, with a cation exchange capacity of 95 mequiv/100 g and an interlayer distance (d_{001}) of 2.4 nm. The decomposition temperature of Cloisite 20A was above 200°C. The $CaCO_3$ particles supplied by Guang Ping Nano Technology Group, China had a size of about 44 nm and were coated with an organic layer of stearic acid, which was evident with X-ray photoelectron spectroscopy. The detailed characterization of the $CaCO_3$ particles can be found in Ref. 5.

Binary and ternary PP-based nanocomposites, namely PP/nanoclay (NPP), PP/$CaCO_3$ (CPP), and PP/nanoclay/$CaCO_3$ (NCPP), with different filler loadings were prepared via melt blending in a Haake mixer, with a rotor speed of 65 rpm. Before mixing, all materials except the antioxidant (Irganox 1010) were dried in an oven at 100°C for 8 h. The mixing temperature was set to be 180°C, which was much lower than the decomposition temperature of the organic coatings in the nanoclay and the $CaCO_3$. The nomenclature of the nanocomposites was subjected to the filler loading. For instance, NPP4 represents that the filler loading of nanoclay was 4 wt % (to the whole composite); CPP2 represents that the filler loading of $CaCO_3$ was 2 wt %; NCPP24 represents that the filler loadings of nanoclay and $CaCO_3$ were 2 and 4 wt %, respectively. In NPP and NCPP, 20 wt % MA-PP was blended in order to increase the compatibility between the PP homopolymer and the organic-modified nanoclay.

Characterization

The dispersion and exfoliation of the nanoparticles in the PP matrix was examined using a transmission electron microscope (TEM; Philips CM20) with an acceleration voltage of 120 kV. The ultrathin sections ($\sim$ 70 nm) were cut using a Leica ultracut-R microtome and collected on 200-mesh copper grids. Wide-angle X-ray diffraction (WAXD; Philips PW1830) with Cu Kα radiation (λ = 0.154 nm) was applied to investigate the extent of intercalation and exfoliation of the nanoclay, and the crystal structure of the PP matrix. The scanning range (2θ) was from 2° to 30° at a rate of 0.05°/s.

The melting and crystallization temperatures of the nanocomposites were determined using differential scanning calorimetry (DSC, Rheometric Scientific DSC SP). The samples were heated from room temperature to 205°C at a rate of 10°C/min and under nitrogen gas protection. After leaving the sample for 1 min for complete melting, the samples were cooled at a rate of 10°C/min. Dynamic mechanical properties of the nanocomposites were evaluated using dynamic mechanical analysis (DMA, TA 2980) at a dual cantilever mode and a frequency of 1 Hz. The rectangular sample used was with a dimensional size of 63 mm $\times$ 12.7 mm $\times$ 3.3 mm. The scanning temperature was from -60°C to 100°C at a rate of 5°C/min.

Mechanical test

The tensile and impact bars were prepared using a vertical injection-molding machine (Morgan Press), according to ASTM-D 638 type IV and ASTM-D 5942, respectively. Prior to the tests, all the samples

were conditioned at (23 ± 2)°C and a relative humidity of 50% ± 5% for 40 h. The tensile tests were carried out using a universal testing machine (MTS SINTECH 10/D) at a crosshead speed of 5 mm/min. The Young's modulus was determined at a 0.5% strain. For each sample, at least five specimens were tested. Notched charpy impact test was conducted at room temperature using an impact tester with a pendulum energy of 0.5 J. Seven specimens of each sample were tested.

RESULTS AND DISCUSSION

Dispersion of nanofillers in PP matrix

To describe the structure of nanoclay, exfoliated, or intercalated, two techniques, namely WAXD and TEM, were widely used.[1] The former can quantitatively identify the interlayer distance of an intercalated structure by monitoring the diffraction peak at low 2θ. However, this method is difficult to describe the spatial distribution of the clay or any structure nonhomogeneities in a nanocomposite. Moreover, in the cases of irregular intercalation with nonuniform interlayer distances, which can be induced by inhomogeneous distribution of surface modifiers and/or heterogeneous intercalation process during melt blending, weak or even no WAXD diffraction peak can be detected, leading to a false and incomplete interpretation of the nanostructure. A qualitative description of detailed nanostructure of the clay can be given through TEM observations. The main disadvantage of TEM is its limited observation regions, which may not be representative of the whole structure in a nanocomposite. Comparing the results obtained with the two aforementioned tools is thereby always suggested.

Figure 1 depicts the WAXD patterns for the natural clay and the nanocomposites. Evidently, the diffraction peak, corresponding to the clay interlayer distance (d_{001}) for all the nanocomposites shifted toward a lower 2θ, compared to the natural clay with an organic modification. In addition, the diffraction peak became much broader, particularly for the nanocomposites with a low clay concentration. These observations suggest that the nanoclay in the nanocomposites was heavily intercalated or partially exfoliated. In other words, with the help of compatibilizer, MA-PP and/or nonpolar PP molecular chains had penetrated into the galleries between clay platelets. These results were in good agreement with other works with the use of MA-PP containing a moderate MA content.[12,20] A moderate MA content makes the MA-PP has a relatively strong interaction capability with organic-modified clay and a required miscibility with PP so that a partially exfoliated structure of the nanoclay can be achieved in PP/clay

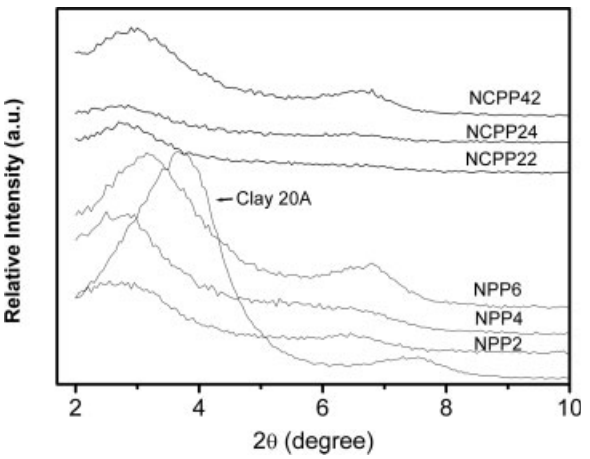

Figure 1 WAXD patterns of the nanoclay and the nanocomposites.

systems.[20] As suggested in Figure 1, the intercalation/exfoliation extent of the clay was dependent on the filler concentrations. In NPP, when the nanoclay content increased from 2 to 6 wt %, the corresponding interlayer distance decreased from 3.5 to 2.8 nm. In NCPP with the incorporation of nano-$CaCO_3$, the clay intercalation/exfoliation extent seemed to be enhanced, which was hinted by the differences in broadness and intensity of the diffraction peaks and also evident by TEM micrographs as discussed later. It has been understood that for a good dispersion of nanoclay, besides the interactions between the nanoclay and the matrix, two other factors, namely mechanical shear stress and molecule diffusion, need to be considered during melt blending.[20,21] High shear stresses facilitate the overcome of kinetic limits associated with the breakup of agglomerated clay particles and the transportation of broken clay platelets. From the point of this view, high matrix viscosity is preferred for a better nanoclay exfoliation, which can be achieved by using polymers with a high molecular weight or adding inorganic particles into the matrix. The former has been experimentally verified[22] and the latter seems plausible from this work. However, it should also be emphasized that, with a high filler concentration, the movement of the molecular chains is constrained and thus the diffusion of the molecular chains into the galleries between clay platelets becomes difficult. As a consequence, the nanoclay intercalation/exfoliation will be deteriorated. The results obtained in this work suggest that using nano-$CaCO_3$ particles may be able to adjust the matrix viscosity and provide a balance between shear stresses and diffusion processes, which finally impart a high level of nanoclay exfoliation.

The nanoclay structure as well as the dispersion of the $CaCO_3$ particles in the nanocomposites were also examined using TEM. As can be seen in Figure 2(a), the TEM micrographs of CPP4, the spherical $CaCO_3$

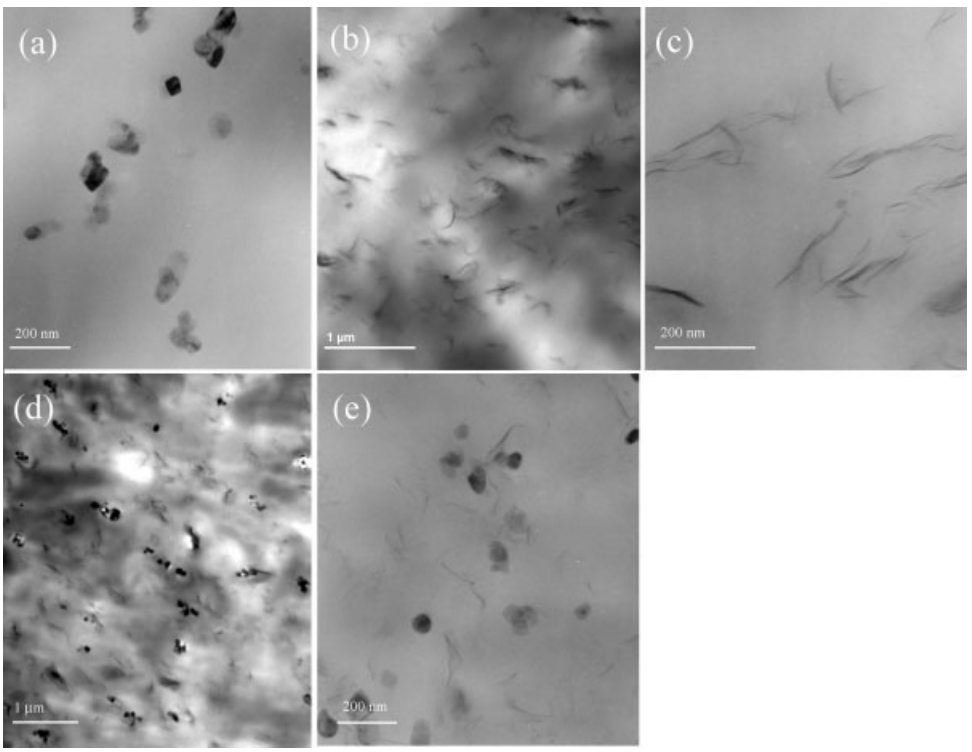

Figure 2 TEM micrographs of the nanocomposites (a) CPP4; (b) and (c) NPP2; (d) and (e) NCPP22.

nanoparticles, were dispersed homogeneously in the matrix without large agglomerates. Figure 2(b,c) shows that the nanoclay in NPP2 was partially exfoliated where the clay tactoids consisted of several to tens platelets was in a disordered structure. This irregularity in interlayer distance was the result of the penetration of PP chains into the clay galleries and it led to the broadening of the diffraction peak in WAXD patterns. In NCPP22, the nanoclay exfoliation extent was evidently much higher than that in NPP2 [cf. Figure 2(d,e)]. Although it is early to declare that this was a fully exfoliated structure, a lot of single platelets and the clay tactoids with two or three platelets can be obviously observed. This enhancement in exfoliation extent of the nanoclay ought to result from the incorporation of $CaCO_3$ particles, which was uniformly embedded in the matrix [cf. Fig. 2(d,e)]. These TEM observations were in good agreement with previous WAXD analysis.

Crystal structure and crystallization behavior

It is known that at least three crystal forms, namely α-, β-, and γ- can be formed for PP.[23] Monoclinic α-phase is generally the predominant crystal structure. Its characteristic peaks (2θ) are located at 14.0°, 16.9°, 18.5°, 21.0°, and 21.8°, corresponding to the crystal planes of (110), (040), (130), (131), and (111), respectively. The formation of β-phase can be encouraged with the addition of β-nucleation particles. Its characteristic peaks, d_{300} and d_{301}, are located at 2θ = 16.2° and 21.0°, respectively. Surface-modified $CaCO_3$ particles have been extensively reported to be able to promote the nucleation of β-phase,[7,24] which was also evident by our WAXD results, as shown in Figure 3, the pattern of CPP4. The β-phase fraction can be estimated by the *K*-value of Jones et al. with the use of the intensity of diffraction peaks, i.e. $K = I_{(300)\beta}/(I_{(300)\beta} + I_{(110)\alpha} + I_{(040)\alpha} + I_{(130)\alpha})$.[25] Accordingly, $K = 1$ for the fully β- and $K = 0$ for the fully α-phase PP. For the current system, the β-phase fraction in CPP was about 40%. Figure 3 also

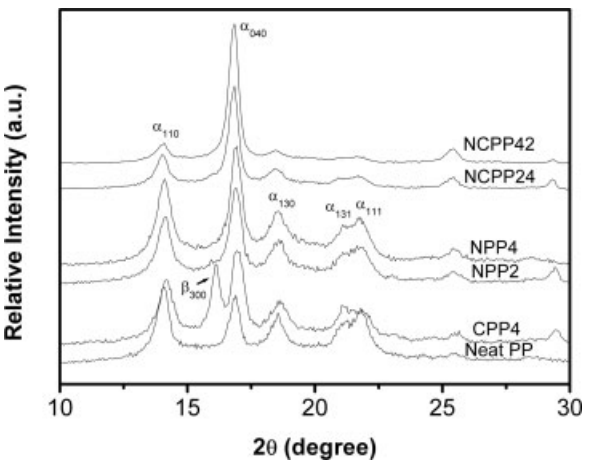

Figure 3 WAXD patterns of the neat PP and the nanocomposites.

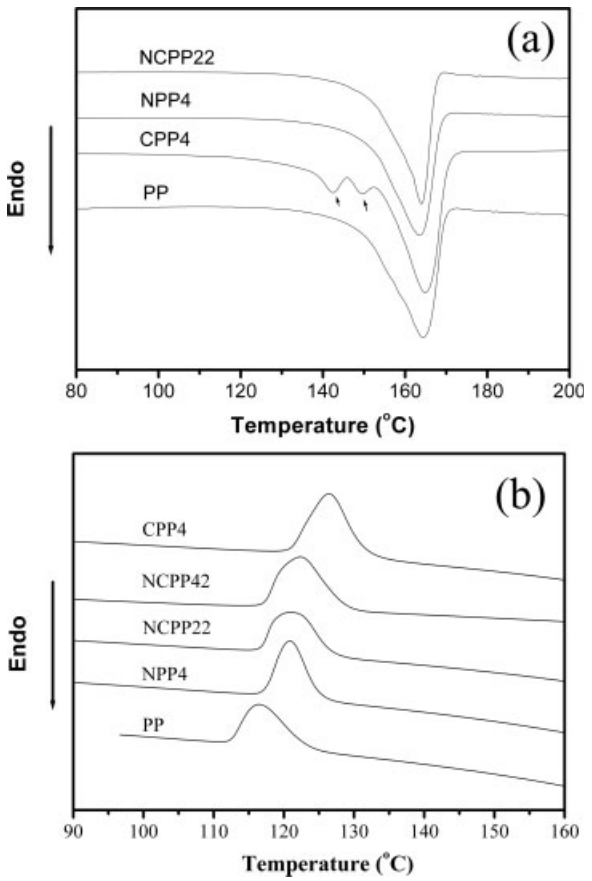

Figure 4 DSC scans of the neat PP and the nanocomposites (a) heating curves; (b) cooling curves.

displays the WAXD patterns of the neat PP, NPP, and NCPP nanocomposites, where only the α-phase diffraction peaks appeared. These observations suggest that the nanoclay did not have the ability to promote the formation of β-phase PP, and the β-nucleation effect of the $CaCO_3$ particles was also inhibited when they coexisted with the nanoclay. This inhibition was very likely because the exfoliated nanoclay had a huge specific surface area and acted as a selective α-nucleating agent, so that the crystallization of the α-phase PP was speeded up significantly and the growth of the β-phase nucleated by the $CaCO_3$ particles was suppressed.

Figure 4(a) presents the DSC heating curves of the neat PP and the nanocomposites. Only one melting peak at about 165°C, corresponding to α-phase PP, was detected for all the samples except CPP. In CPP, as indicated by arrows in Figure 4 multiple melting took place, which was an indication of the presence of β-phase PP.[5] These results suggest that $CaCO_3$ had a nucleation effect on the formation of β-phase PP, but this effect would be preserved when it coexisted with nanoclay. These phenomena were consistent with the WAXD data. Table I summarizes the crystallinity and the crystallization temperatures of these samples. Evidently, with the addition of nanoclay and/or $CaCO_3$ the crystallinity of the PP matrix was not significantly varied while the crystallization temperatures were increased by 2 ~ 5°C for nanoclay and ~ 10°C for $CaCO_3$ [cf. Fig. 4(b)]. Although it was reported that the platy filler particles had two magnitudes more nucleation sites per unit surface area of the minerals than that of spherical $CaCO_3$ particles,[26] the exfoliated structure of the nanoclay greatly restrict the movement of the molecular chains, which would retard the crystallization of the matrix and lead to a lower increase in crystallization temperature.[27] Therefore, the $CaCO_3$ particles seemed to be more effective for promoting the nucleation and growth of crystalline phase in the PP binary nanocomposites. However, when the $CaCO_3$ particles was compounded with the nanoclay in the PP matrix, namely in NCPP, the nucleation effect of $CaCO_3$ was suppressed, which was believed to be caused by the different nucleation sites between these two particles and the restriction of molecular chain movement.

Mechanical property

The mechanical properties of the nanocomposites were investigated by using DMA, tensile, and impact tests. Figure 5 shows the storage modulus of the nanocomposites as a function of temperature. It can be seen that with the incorporation of the nanoparticles, the storage modulus of the nanocomposites was dramatically increased within the entire test temperature range. Obviously, the reinforcing effect of the nanoclay was superior to $CaCO_3$ at a same filler concentration such as 4 wt %. This phenomenon was generally ascribed to the large aspect ratio of exfoliated clay. Most interestingly, when adding both nanoparticles simultaneously, much higher moduli were obtained, which should resulted from the better exfoliation of the nanoclay as discussed previously. The variations of stiffness of the nanocomposites with the nanoparticles were further confirmed with tensile tests, conducted at room temper-

TABLE I
Melting and Crystallization Temperatures of the Neat PP and the Nanocomposites (X_c Was Calculated by Taking 170 J/g to be the Standard Heat of PP Crystallization[5])

Sample	T_m (°C)	X_c (%)	T_c (°C)
PP	165	53	116
CPP4	142, 150, 164	53	126
NPP2	165	53	120
NPP4	164	54	121
NPP6	163	50	118
NCPP22	164	54	121
NCPP24	164	50	120
NCPP42	163	48	120

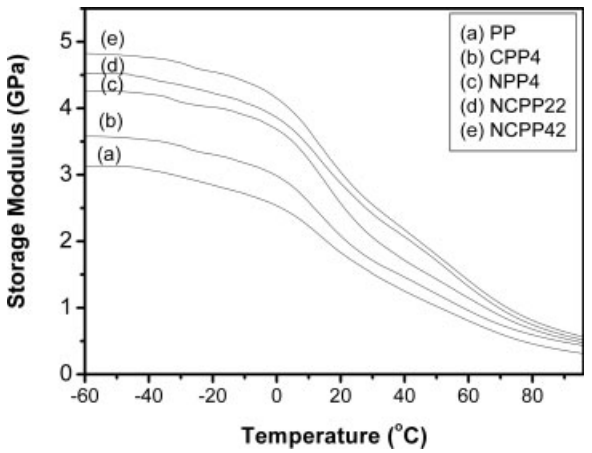

Figure 5 Storage modulus of the neat PP and the nanocomposites as a function of temperature.

ature. The results are shown in Figure 6. Evidently, the highest stiffness of the nanocomposites was attained when blending the PP with both nanoclay and $CaCO_3$ particles [cf. Fig. 6(a)].

Figure 6(b) presents the changes of the yield stress of the nanocomposites. In CPP, the yield stress was less changed, and a slight decrease occurred at a high filler loading. This phenomenon can be attributed to the nucleation effect of the $CaCO_3$ particles and the weak interfacial interactions between the $CaCO_3$ particles and the PP matrix. The former reduced the spherulite size and thus the yield stress.[5] The latter made it possible for the occurrence of debonding at the particle/matrix boundary before yielding.[6] Differing from CPP, in NPP the yield stress was increased considerably, which suggests that the interfacial interaction between the nanoclay and the matrix was quite good. The good interfacial interaction should be benefited from the use of MA-PP as compatibilizer. In NCPP, the yield stress was almost the same as that in NPP although a slight increase was found. This comparable yield stress between NCPP and NPP was believed to be a result of two counter balance effects associated with the addition of $CaCO_3$ in NPP. One was the enhanced exfoliation extent, leading to a higher yield stress, and the other was the detrimental effect of the $CaCO_3$ particles on the yield stress.

The variations of notched impact strength of the nanocomposites are illustrated in Figure 6(c). In accordance with other reports, the incorporation of $CaCO_3$ effectively improved the impact strength. For instance, the increase was more than 50% when 4 wt % $CaCO_3$ was added. According to literature review,[4–8,24] the main toughening mechanisms of PP/$CaCO_3$ nanocomposites can be summarized as (1) crack deflection; (2) reduction in spherulite size due to the nucleation effect of the nanoparticles; (3) formation of β-phase crystallites, which is believed to have a higher impact resistance than α-phase crystallites[28]; (4) occurrence of interfacial debonding between the particles and the matrix, which can release the triaxial stress constraint at the crack tip and subsequently trigger massive plastic deformation of the matrix around the particles. In the current case, it seems that the mechanism of debonding and subsequent matrix plastic deformation did not occur, as indicated by the SEM micrograph shown in Figure 7(b), which was taken at the fracture surface of a CPP4

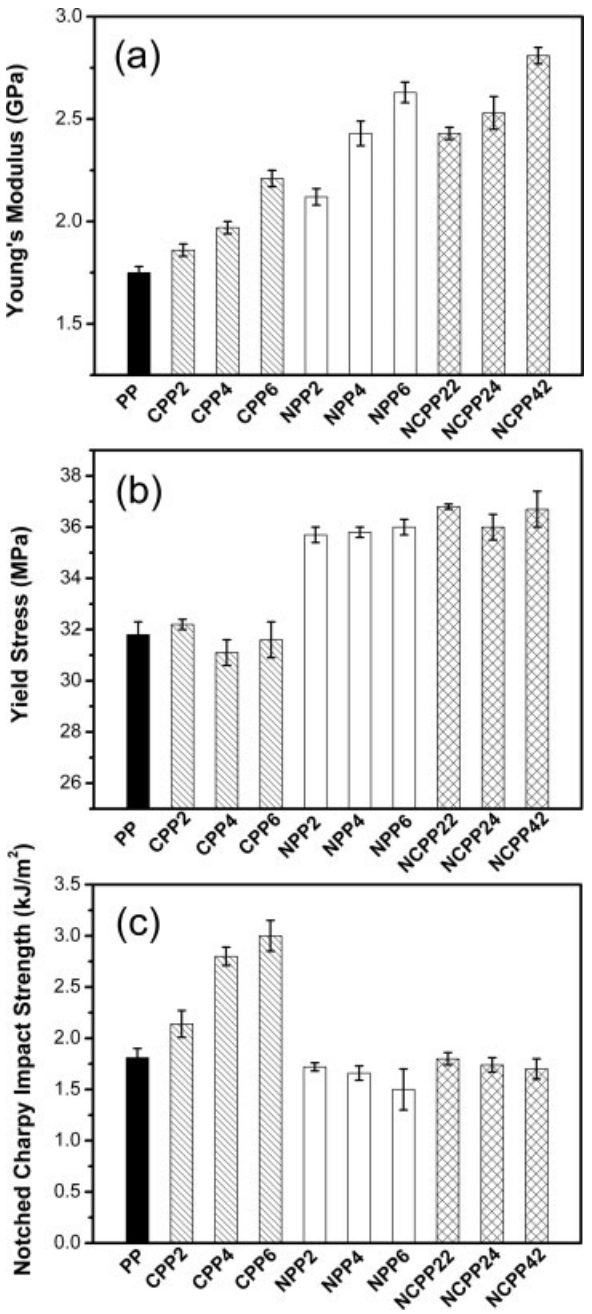

Figure 6 Mechanical properties of the neat PP and nanocomposites obtained at room temperature. (a) Young's modulus; (b) yield stress; (c) notched charpy impact strength.

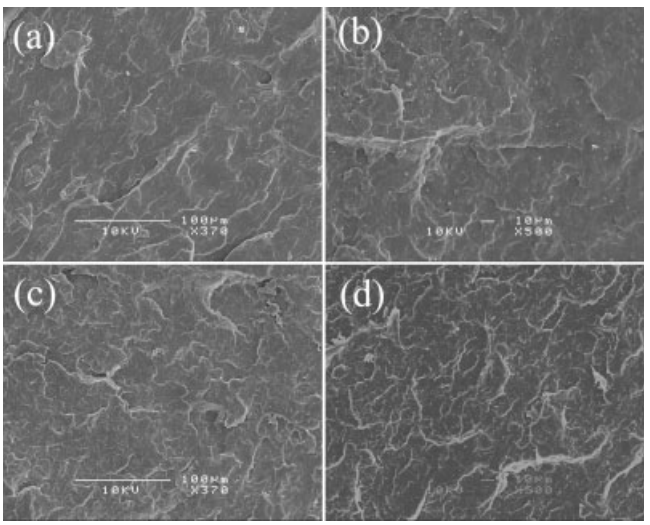

Figure 7 SEM micrographs taken on the fracture surface of the nanocomposites. (a) Neat PP; (b) CPP4; (c) NPP2; (d) NCPP22.

specimen. Moreover, because of the small size of the $CaCO_3$ particles, the occurrence of crack deflection became impractical. Thus, the enhancement in impact strength for the current CPP nanocomposites can be ascribed to the reduction in spherulite size and the formation of β-phase PP. In NPP, the impact strength was severely weakened and gradually decreased with increasing the clay concentration. As shown in Figure 7(c), the fracture surface of NPP was featureless, indicating a rather brittle fracture. This decrease in impact strength was considered to be caused by the presence of partially exfoliated nanoclay, which restricted the flexibility of the matrix molecules and thus the degree of plastic deformation. Another possible embrittlement mechanism proposed by Cotterell et al.[29] recently is that because of the large aspect ratio of the nanoclay and its orientation, multiple crazing happening ahead of the crack tip during fracture may be inhibited, making semicrystalline polymers such as PP embrittled.

In NCPP, although the impact strength was slightly increased when compared to NPP, this increase was much less than our expected value. As shown in Figure 7(d), the fracture surface of NCPP exhibited a higher density of stress-whitening site than that of NPP, which was believed to be a result of their different clay exfoliation extents. Because of the different Young's modulus and Poisson's ratio of the nanoclay and the PP matrix, exfoliated clay platelets became stress concentrators when subjected to a load, which finally resulted in stress-whitening on the fracture surface. Therefore, the higher the exfoliation extent, the denser stress-whitening sites were. Although the fracture surface of NCPP had a minor difference from that of NPP, it was also featureless and brittle-like. This brittle feature suggests that the $CaCO_3$ particles in NCPP did not show any toughening effect as they did in CPP. This difference should be resulted from the different crystallization behaviors in CPP and NCPP. As discussed previously, in NCPP the crystallization behavior was dominated by the nanoclay, so that the nucleation effect of $CaCO_3$ was suppressed and no β-phase crystallites were formed. Consequently, the toughening mechanisms raised by $CaCO_3$ particles in CPP became ineffective in NCPP. Moreover, similar as CPP, in NCPP interfacial debonding between the $CaCO_3$ particles and the matrix seemed not to take place, and no localized plastic deformation occurred in the matrix at the vicinity of the $CaCO_3$ particles. As a result, the impact strength and fracture surface in NCPP were comparable to those in NPP. It can therefore be concluded that with the coexistence of the $CaCO_3$ and nanoclay particles, although the stiffness of the nanocomposites can be effectively improved, the toughening mechanisms of $CaCO_3$ particles associated with its nucleation effects including spherulite size reduction and β-phase formation will no longer take effect. In the future, the efforts should be taken to promote the most important toughening mechanism of spherical $CaCO_3$ nanoparticles, i.e. particle debonding and subsequent shear deformation of interparticle matrix ligament, to take place in the ternary NCPP nanocomposites.

CONCLUSION

Binary and ternary PP-based nanocomposites with nanoclay and nanosized $CaCO_3$ particles were prepared via melt blending. With the addition of $CaCO_3$ in NCPP, the exfoliation extent of the nanoclay particles was substantially enhanced. Much higher moduli and yield stresses were thereby resulted. The impact strength in NCPP was, however, not significantly increased. The toughening effects of $CaCO_3$ particles observed in CPP seemed to be ineffective in NCPP, which was attributed to the following fact. The crystallization behavior in NCPP was dominated by the partially exfoliated nanoclay which had a huge specific surface area, so that the nucleation effect of $CaCO_3$ was inhibited and no β-phase PP crystallites were formed. In addition, the mechanisms of crack pinning, particle debonding, and subsequent matrix shear deformation were not observed in both CPP and NCPP. The fracture behavior in NCPP was therefore similar to that in NPP, leading to their comparable impact resistances.

The assistance from Materials Characterization and Preparation Facility (MCPF) and Advanced Engineering Materials Facility (AEMF) of HKUST for sample preparation and characterization is highly appreciated. The authors also

need express great thanks to Southern Clay Products (Gonzales, TX) and Guang Ping Nano Technology Group Ltd., China for providing the clay and $CaCO_3$ particles.

References

1. Alexandre, M.; Dubois, P. Mater Sci Eng R 2000, 28, 1.
2. Tjong, S. C.; Meng, Y. Z.; Hay, A. S. Chem Mater 2002, 14, 44.
3. Rong, M. Z.; Zhang, M. Q.; Zheng, Y. Z.; Zeng, H. M.; Walter, R.; Friedrich, K. Polymer 2001, 42, 167.
4. Weon, J. I.; Sue, H. J. J Mater Sci 2006, 41, 2291.
5. Chan, C. M.; Wu, J. S.; Li, J. X.; Cheung, Y. K. Polymer 2002, 43, 2981.
6. Zuiderduin, W. C. J.; Westzaan, C.; Huetink, J.; Gaymans, R. J. Polymer 2003, 44, 261.
7. Thio, Y. S.; Argon, A. S.; Cohen, R. E.; Weinberg, M. Polymer 2002, 43, 3661.
8. Zhang, Q. X.; Yu, Z. Z.; Xie, X. L.; Mai, Y. W. Polymer 2004, 45, 5985.
9. Tjong, S. C. Mater Sci Eng R 2006, 53, 73.
10. Strawhecker, K. E.; Manias, E. Chem Mater 2000, 12, 2943.
11. Cho, J. W.; Paul, D. R. Polymer 2001, 42, 1083.
12. Kawasumi, M.; Hasegawa, N.; Kato, M.; Usuki, A.; Okada, A. Macromolecules 1997, 30, 6333.
13. Reichert, P.; Nitz, H.; Klinke, S.; Brandsch, R.; Thomann, R.; Mulhaupt, R. Macromol Mater Eng 2000, 275, 8.
14. Hasegawa, N.; Kawasumi, M.; Kato, M.; Usuki, A.; Okada, A. J Appl Polym Sci 1998, 67, 87.
15. Svoboda, P.; Zeng, C. C.; Wang, H.; Lee, J.; Tomasko, D. L. J Appl Polym Sci 2002, 85, 1562.
16. Chen, L.; Wong, S. C.; Pisharath, S. J Appl Polym Sci 2003, 88, 3298.
17. Liang, J. Z.; Li, R. K. Y. J Appl Polym Sci 2000, 77, 409.
18. Li, Y. M.; Wei, G. X.; Sue, H. J. J Mater Sci 2002, 37, 2447.
19. Lim, J. W.; Hassan, A.; Rahmat, A. R.; Wahit, M. U. J Appl Polym Sci 2006, 99, 3441.
20. Kim, K. N.; Kim, H.; Lee, J. W. Polym Eng Sci 2001, 41, 1963.
21. Bousmina, M. Macromolecules 2006, 39, 4259.
22. Fornes, T. D.; Yoon, P. J.; Keskkula, H.; Paul, D. R. Polymer 2001, 42, 9929.
23. Karger-Kocsis, J. Polypropylene: Structure, Blends and Composites; Chapman & Hall: New York, 1995.
24. Wan, W. T.; Yu, D. M.; Xie, Y. C.; Guo, X. S.; Zhou, W. D.; Cao, J. P. J Appl Polym Sci 2006, 102, 3480.
25. Jones, T. A.; Aizlewood, J. M.; Beckett, D. R. Macromol Chem 1964, 75, 134.
26. McGenity, P. M.; Hooper, J. J.; Paynter, C. D.; Riley, A. M.; Nutbeem, C.; Elton, N. J.; Adams, J. M. Polymer 1992, 33, 5215.
27. Wang, K.; Liang, S.; Deng, J. N.; Yang, H.; Zhang, Q.; Fu, Q.; Dong, X.; Wang, D. J.; Han, C. C. Polymer 2006, 47, 7131.
28. Chen, H. B.; Karger-Kocsis, J.; Wu, J. S.; Varga, J. Polymer 2002, 43, 6505.
29. Cotterell, B.; Chia, J. Y. H.; Hbaieb, K. Eng Fract Mech 2007, 74, 1054.